Journal of Alloys and Compounds 503 (2010) 170–176

Contents lists available at ScienceDirect

Journal of Alloys and Compounds

journal homepage: www.elsevier.com/locate/jallcom

Properties of CdS films deposited by the electron beam evaporation technique

K. Sivaramamoorthy[a], S. Asath Bahadur[a,b], M. Kottaisamy[a,c], K.R. Murali[a,d,*]

[a] Department of Physics, Rajapalayam Rajus College, Rajapalayam, Tamilnadu, India
[b] Department of Physics, Kalasalingam University, Krishnan Koil, Tamilnadu, India
[c] Department of Chemistry, Kalasalingam University, Krishnan Koil, Tamilnadu, India
[d] Electrochemical Materials Science Division,[1] CECRI, Karaikudi, Tamilnadu, India

ARTICLE INFO

Article history:
Received 19 December 2009
Received in revised form 29 April 2010
Accepted 30 April 2010
Available online 6 May 2010

Keywords:
Semiconductors
II–VI
Thin films
Electronic materials

ABSTRACT

Thin CdS films were electron beam evaporated. The CdS powder synthesized in the laboratory by a chemical method was used as source for the deposition of films. Clean glass substrates were used. The substrate temperature was varied in the range of 30–250 °C. X-ray diffraction studies indicated polycrystalline hexagonal structure. The band gap was 2.39 eV. The grain size was 25–35 nm and the surface roughness was 0.3–1.5 nm with increase of substrate temperature. Photoconductive cells fabricated with the doped and undoped films have exhibited high photosensitivity and high signal to noise ratio. The current voltage characteristics were linear.

1. Introduction

Cadmium sulphide (CdS), due to its wide band gap, photoconductivity, and high electron affinity, is known to be an excellent heterojunction partner for p-type cadmium telluride, p-type copper indium diselenide. It has been widely used as a window material in high efficiency thin film solar cells based on cadmium telluride or copper indium diselenide and in photoelectrochemical solar cells [1–3]. CdS is a semiconducting material useful for printed electronics [4]. It is an interesting crystal material in the area of photodetectors, semiconductor lasers, and nonlinear integrated optical devices. The importance of wide band gap materials is related to the possibility of fabricating light emitting diodes or laser heterostructures for emission in the visible spectral range. These devices are important for many applications. For example, they are useful in medical diagnosis and for fabricating red–green–blue display and as down shifting layer for silicon solar cells [5–8]. CdS thin films can be deposited by different deposition techniques such as chemical bath deposition, vacuum evaporation, spray pyrolysis, thermal evaporation, chemical vapor deposition, metal organic vapor-phase epitaxy, close space vapor transport, photochemical deposition, radio frequency sputtering, vapor transport deposition, screen printing, electro deposition, pulsed laser deposition [9–17] and chemical bath deposition [18]. In the present work, thin films of CdS were deposited by the electron beam evaporation technique using the laboratory synthesized CdS powder as the source.

2. Experimental methods

CdS powder was synthesized in the laboratory by the following method. 80 g of cadmium acetate was dissolved in 200 ml of triple distilled water, and 50 g of thiourea was dissolved in 250 ml of triple distilled water by gentle warming. This solution was filtered after cooling. The cadmium acetate solution was taken in a three litre round bottomed Pyrex flask fitted with ground joints, and 150 ml of fresh ammonia (specific gravity 0.91) was added when a clear solution was obtained. Thiourea solution was mixed with 150 ml of ammonia and added to the clear cadmium ammonia complex and refluxed on a heating mantle at 80 °C, provided with a facility for magnetically stirring the contents, for 2 h. 30 ml of ammonia was added at intervals of 30 min. The solution turned canary yellow in colour at the beginning, a little later, shining tiny crystals of cadmium sulphide are noticed in the solution as well as on the walls of the flask and finally the bulk precipitate of cadmium sulphide turned to a bright orange hue. The heating is stopped and the precipitate was allowed to age for 12–16 h. It was filtered through a Buchner funnel with Whatmann 42 filter paper using rotary vacuum suction provided with requisite traps to avoid pump oil vapor contaminating the powder. The precipitate was washed with hot (~70 °C) acetic acid solution to remove traces of hydroxide/oxide of cadmium that may still be present. Further washings were effected with triple distilled water till the filtrate showed neutral pH and finally washed with pure ethanol. The precipitate was dried in vacuum oven and stored in a vacuum desiccator.

The apparent reactions without going into mechanism are:

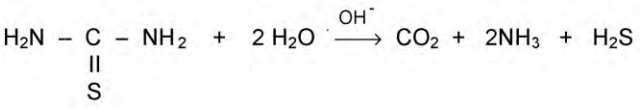

* Corresponding author at: Electrochemical Materials Science Division, CECRI, Karaikudi, Tamilnadu 630 006, India. Tel.: +91 4565 224502.
E-mail address: muraliramkrish@gmail.com (K.R. Murali).
[1] Council of Scientific and Industrial Research, New Delhi, India.

0925-8388/$ – see front matter © 2010 Elsevier B.V. All rights reserved.
doi:10.1016/j.jallcom.2010.04.227

Table 1
AAS analysis of the CdS powders.

Sample	Impurity content (ppm)							
	Cu	Fe	Ca	K	Na	Zn	Pb	Co
CdS (prepared)	10	20	20	2	2	–	–	–
CdS (Kochlight)	–	22	95	7	6	2	5	2

$$Cd(NH_3)_4(OAc)_2 + H_2S \rightarrow CdS + 2NH_4OAc$$

Thin CdS films were deposited using a Hind Hivac coating unit. A vacuum better than 8×10^{-6} Torr was used during evaporation. The films were deposited at an operating voltage of 10 kV and a beam current of 10 mA. The source to substrate distance was maintained as 15 cm. The CdS powder synthesized in the laboratory was used for the deposition of films. Glass substrate coated with tin oxide of 5 Ω/□ were used. The substrate temperature was varied in the range of 30–250 °C. Indium ohmic contacts were provided on the edges of the surface of the films for photoconductivity measurements. A 250 W tungsten halogen lamp was used for photoconductivity measurements. Spectral response measurements were made using photophysics monochromator. Copper doping was done by dipping the films for 5 min in $CuCl_2$ solution of different concentrations in the range of 0.001–0.011 M. After dipping the films were annealed in air at 450 °C for10 min. Noise characteristics of the doped and undoped photoconductive films were studied as follows. The load resistance was adjusted to a value equal to the resistance of the photoconductive film. The power supply was switched ON and in the absence of an applied bias voltage, the signal across the cell was measured; this represents the noise signal due to the power supply. Next the chopper was switched ON and maintaining the light in the OFF condition, the signal was measured across the cell. This value gives the total noise signal due to chopper and power supply. After this, the light was switched ON, this causes the resistance of the film to decrease. When light is incident on the cell, an increase in voltage drop occurs across the load resistance. The AC signal across the cell on illumination is measured and the signal to noise ratio (SNR) is calculated from the signal and noise signal values.

Thin CdS films were deposited on cleaned glass substrates maintained at different temperatures in the range 30–300 °C. Thickness of the films estimated using Mitutoyo surface profilometer was in the range of 0.8–1.4 μm with decrease of substrate temperature. For electrical measurements indium was evaporated on both the ends of the film surface.

3. Results and discussion

Atomic absorption spectrometry was used to determine the purity of the powder. The purity of the synthesized powder was comparable to the commercially available AR grade Koch light powder (Table 1). The content of Cd and S is 52% and 48%, respectively, for the laboratory synthesized powder and Koch light powder, the composition was Cd (51%) and S (49%). The X-ray diffraction (XRD) pattern of the CdS powder exhibited all the peaks corresponding to the hexagonal phase. X-ray diffraction (XRD) patterns of cadmium sulphide films deposited on titanium substrates at different temperatures in the range 30–300 °C are shown in Fig. 1. Studies were made on the films coated on titanium substrates, since these films were used for photoelectrochemical cell studies. Films deposited on glass substrates also exhibited the same peaks but the intensities of the peaks were lower than for the films deposited on titanium substrates. It is observed from the figure that the films are polycrystalline exhibiting the hexagonal structure. As the substrate temperature increased, the intensity of the peaks increased and the width of the peaks decreased indicating the formation of larger crystallites at higher substrate temperature. The peaks corresponding to (1 0 0), (0 0 2), (1 0 1), (1 0 2), (1 1 0), (1 0 3) and (1 1 2) reflections were observed (JCPDS 6-314). The crystallite size determined using the Scherer's equation was 12 nm, 16 nm, 24 nm and 30 nm for the films deposited at different substrate temperatures of 30 °C, 100 °C, 200 °C and 300 °C, respectively. The films deposited at a substrate temperature of 300 °C were post-heat treated in air for 10 min at different temperatures in the range 450–550 °C for photoconductivity experiments. The XRD pattern of the films post-heat treated in air at different temperatures are shown in Fig. 2. Peaks corresponding to the hexagonal phase were observed. As the heat

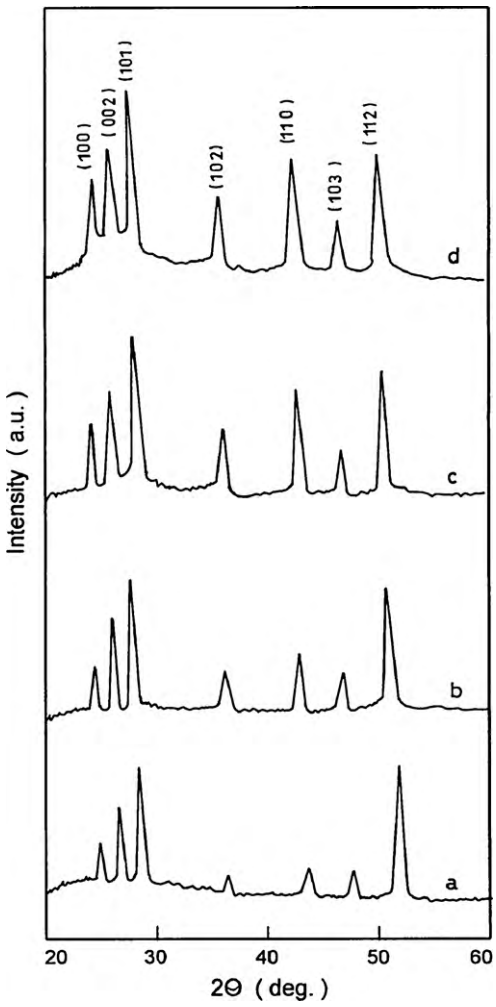

Fig. 1. XRD pattern of CdS films deposited at different substrate temperatures: (a) 30 °C, (b) 100 °C, (c) 200 °C and (d) 300 °C.

treatment temperature increases, the crystallinity of the films also increased as evidenced by the sharpness of the XRD peaks. Peaks corresponding to (1 0 0), (0 0 2), (1 0 1), (1 0 2), (1 1 0), (1 0 3) and (1 1 2) reflections were observed.

The structural parameters, such as lattice constant, internal stress and dislocation density, were calculated from the XRD data

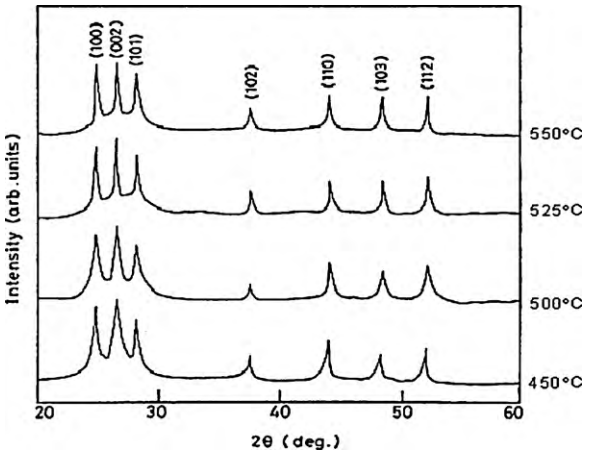

Fig. 2. XRD patterns of the CdS films deposited at a substrate temperature of 300 °C and post-heated in air at different temperatures.

Table 2
Structural parameters of CdS films.

Substrate temp. (°C)	Lattice spacing (Å) (1 0 1 peak)	Lattice parameters (Å)		Internal stress (GPa)	Dislocation density (10^{15} lines m^{-1})
		(*a*)	(*c*)		
30	3.16	4.10	6.71	−0.21	4.3
100	3.17	4.11	6.72	−0.14	2.8
200	3.18	4.12	6.73	−0.11	1.9
300	3.19	4.13	6.74	−0.06	0.6

for CdS films, and their variation as a function of substrate temperature was studied. The lattice parameter '*a*' and '*c*' for hexagonal CdS film was calculated using the relation

$$1/d^2 = 4/3(h^2 + hk + k^2)/a^2 + l^2/c^2$$

where *h*, *k*, *l* are the lattice planes and *d* is the interplanar spacing determined using Bragg's equation. The variation of the lattice constant with the deposition temperature is presented in Table 2. The lattice constant increased with substrate temperature. The change of lattice constant with substrate temperature clearly indicated that the crystallites were under stress, leading to either elongation or compression of the lattice constant. This might be due to the change of density and nature of native imperfections with the deposition temperature of the film [19]. In general, all polycrystalline thin films are in a state of stress irrespective of their preparation technique. The total stress present in the films is equal to the sum of thermal stress and intrinsic stress in the absence of an applied external stress:

$$\sigma_{\text{Total}} = \sigma_{\text{Thermal}} + \sigma_{\text{Intrinsic}}$$

The difference in thermal expansion coefficients of substrate and film gives rise to thermal stress, whereas the difference in lattice constant from that of bulk led to the development of intrinsic stress in the film. In our present study, the thermal stress is calculated using the following relation [20]

$$\sigma_{\text{Thermal}} = (\alpha_{\text{CdS}} - \alpha_{\text{Titanium}})\Delta TY$$

where $\alpha_{\text{CdS}} = 7.034 \times 10^{-6}/^{\circ}\text{C}$ [21] and $\alpha_{\text{Titanium}} = 8.04 \times 10^{-6}/^{\circ}\text{C}$ are the thermal expansion coefficients of CdS and titanium, respectively. *Y* is Young's modulus of CdS and ΔT is the temperature of the CdS film during the formation minus the temperature at measurement. The evaluated thermal stress was found to be compressive in nature, and varied in the range of 7–12% of the total stress with the increase of deposition temperature. The internal stress in CdS films was determined using the difference in lattice constants of the film and bulk material using the relation [22]

$$\sigma_{\text{Intrinsic}} = Y(a - a_0)/2\gamma a_0$$

Here, '*a*' is the lattice constant measured from the XRD, a_0 is the bulk lattice constant and γ is Poisson's ratio. The variation of internal stress with deposition temperature is presented in Table 2. The dislocation density (δ) was determined using the relation [23]

$$\delta = 15\beta \cos\theta/4aD$$

where 'β' is the full width at half maximum, '*a*' is the lattice parameter, '*D*' is the grain size and 'θ' is the Bragg angle. The variation of dislocation density with substrate temperature is also indicated in Table 2. It was observed that the dislocation density decreased with the increase of deposition temperature. This might be due to the improvement in crystallinity.

Fig. 3 shows the binding energies of the Cd ($3d_{5/2}$ and $3d_{3/2}$) and S ($3d_{5/2}$ and $3d_{3/2}$) levels of the CdS films annealed at different temperatures. There is no preferential removal of Cd on annealing, but a small amount of S is lost by evaporation. This is also evidenced from the EDAX results. As shown in the figure, the peak energy levels associated with the Cd ($3d_{5/2}$ and $3d_{3/2}$) appeared at 405 eV and 411.7 eV, respectively, these values are in close agreement with the literature values. Fig. 3 also shows the binding energies of S ($3d_{5/2}$ and $3d_{3/2}$) levels at 168.0 eV and 170.0 eV, respectively.

Surface morphology of the films deposited at different substrate temperatures are shown in Fig. 4. The average surface roughness and the grain size observed by AFM were in the range 0.3–1.5 nm and 25–35 nm, respectively. The standard deviation of the roughness and grain size of each material is large; hence, there is no significant dependence of these parameters on the material type. The average crystallite size determined by the Scherrer formula from the XRD data was smaller by approximately 10% compared to the average grain size determined by the AFM. This could be attributed to the fact that the AFM measurement is more sensitive to the surface structure and that of the XRD is sensitive to the structure of the film bulk. In addition, as the crystallites columns that grow during the deposition tend to have a larger diameter

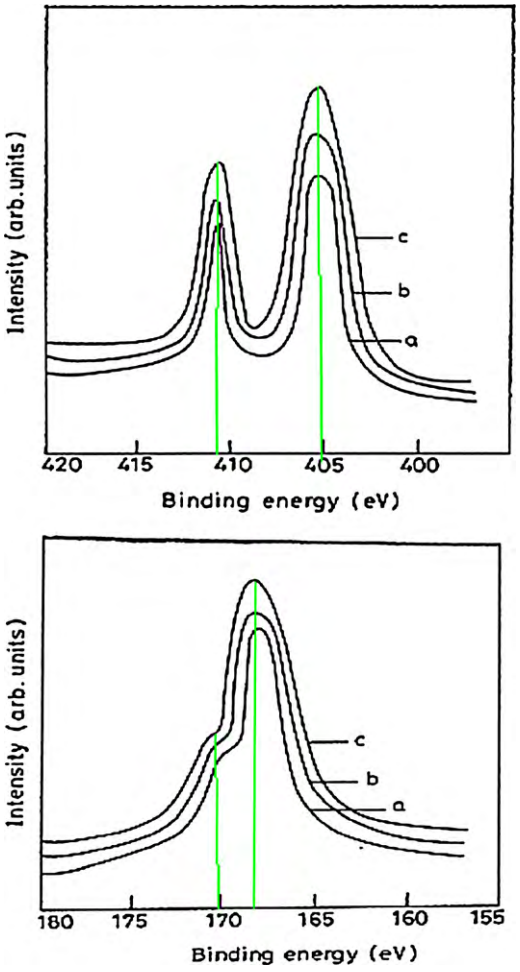

Fig. 3. XPS spectra of Cd and S in CdS films deposited at a substrate temperature of 300 °C and post-heated at different temperatures in air: (a) 450 °C, (b) 500 °C and (c) 550 °C.

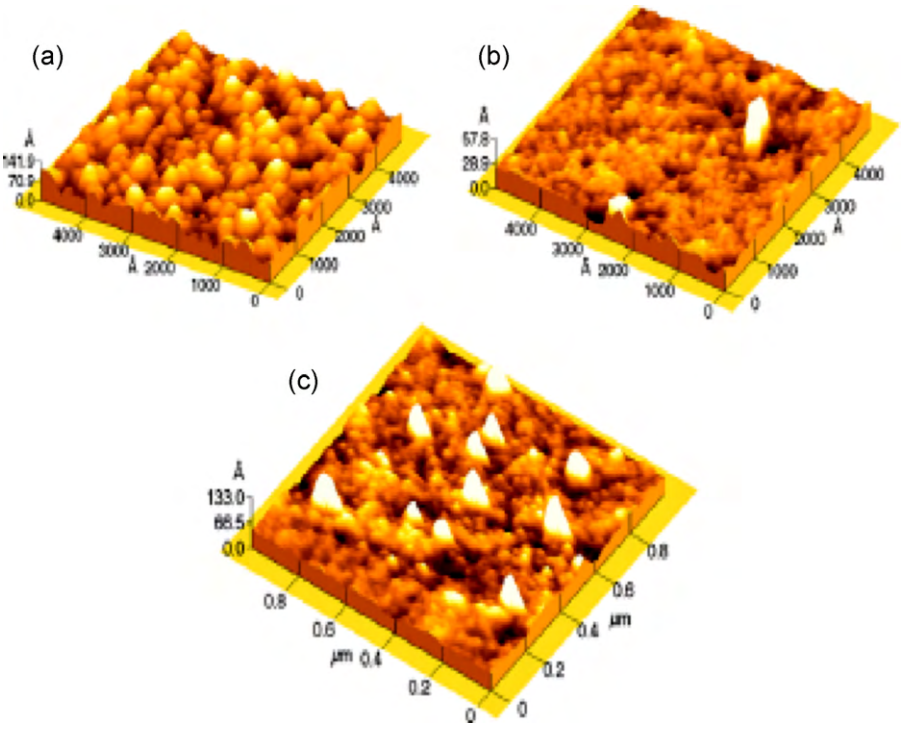

Fig. 4. Atomic force microscopic image of the CdS films deposited at different temperatures: (a) 300 °C, (b) 100 °C and (c) 200 °C.

at the surface, the surface grains have a larger average crystallite size.

The magnitude of the resistivity varies from 0.1 Ω cm to 20 Ω cm as the substrate temperature is increased and the carrier concentration decreases from 3×10^{18} cm^{-3} to 0.8×10^{17} cm^{-3} with increase of substrate temperature.

The resistivity increase with increase of substrate temperature indicates that the film stoichiometry (excess cadmium or sulphur vacancy, which are electron donor sites that provide additional carriers and reduce the resistivity) plays a dominant role. This can be understood from the fact that CdS films dissociate during annealing by evaporation modifying the Cd/S ratio. Further during annealing, oxygen fills the sulphur vacancies in CdS and as these donor sites are eliminated, the free carrier concentration is reduced at higher temperatures. Invariably the absorbed oxygen results in an increase of film resistivity. The grain boundaries in these films also play a role in controlling the electrical properties. Traps at the grain boundaries in these films are also responsible for the potential barrier that limits carrier mobility.

Optical band gap of the CdS films annealed at 550 °C was determined by measuring the absorbance spectra. The energy gap obtained by extrapolating the linear portion of the $(\alpha h\nu)^2$ vs hν plot (Fig. 5) to the energy axis yielded a direct band gap value of 2.39 eV. This value is in good agreement with earlier reports on thin CdS films.

Fig. 6 shows the variation of photosensitivity (PS) with substrate temperature. It is observed that the films deposited at a substrate temperature of 300 °C, exhibited the maximum photosensitivity, hence further studies were carried out on these films. The photosensitivity was calculated using the following relation

$$PS = (R_D - R_L)/R_D$$

Fig. 7 shows the variation of photosensitivity with intensity of illumination for the cells prepared by using the powder synthesized in the laboratory. It was observed from the figure, as the intensity of illumination increases, the corresponding photosensitivity also increases. Of all the annealing temperatures, the cells prepared with films annealed at 550 °C exhibited maximum photosensitivity. The dependence of PS on light intensity at room temperature can be described in terms of the oxygen absorption effects at high annealing temperatures. The thermal release of oxygen from the surface is the possible mechanism, which is always dominant for cells annealed in argon containing ppm of oxygen and hence both the dark and the photoconductivity are increased. The argon used in the present studies was 99% pure containing ppm of oxygen. The increase in photosensitivity may be due to the creation of oppo-

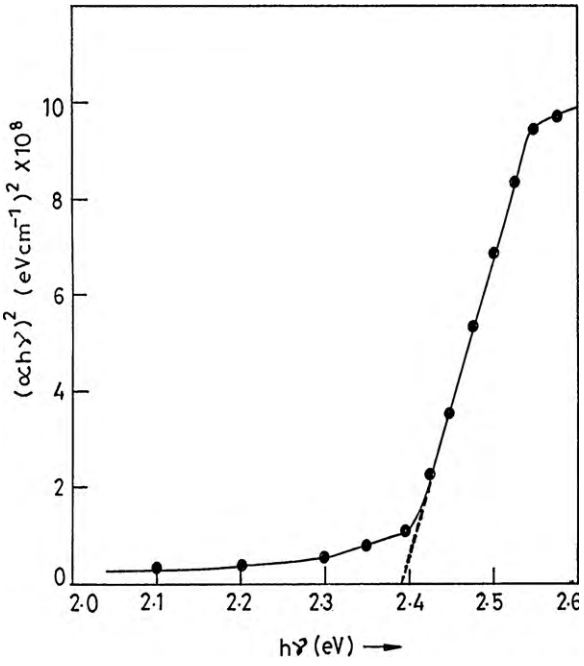

Fig. 5. $(\alpha h\nu)^2$ vs $h\nu$ plot of the CdS films deposited at a substrate temperature of 300 °C.

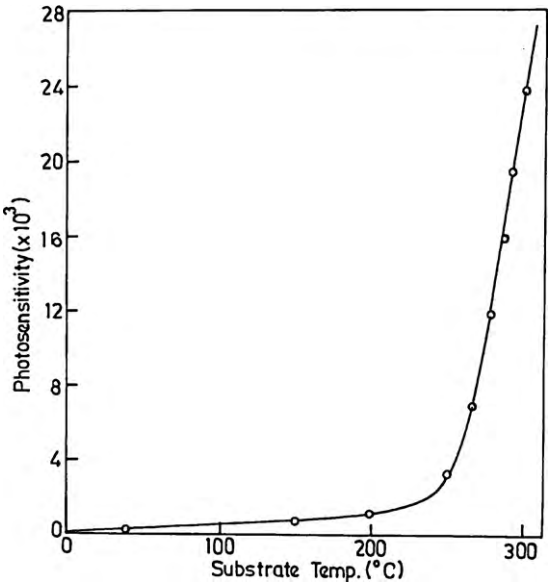

Fig. 6. Variation of photosensitivity with substrate temperature.

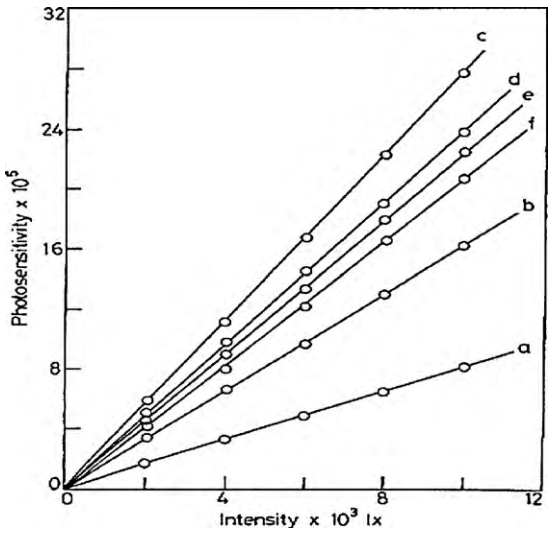

Fig. 8. Dependence of photosensitivity on illumination intensity for doped CdS films deposited at a substrate temperature of 300 °C and post-heated in air at 550 °C and doped with different concentrations of copper: (a) 0.001 M, (b) 0.003 M, (c) 0.005 M, (d) 0.007 M, (e) 0.009 M and (f) 0.011 M.

site type of charge carriers in n-type CdS, as oxygen acts here as an acceptor impurity. Similar behaviour has also been observed in CdS photocells. It was reported that CdS films annealed at lower temperatures contained larger electron concentrations because of a slight excess of Cd, and the carrier concentration did not change appreciably on illumination to exhibit maximum photosensitivity, hence further studies were made only on the films annealed at 550 °C.

Fig. 8 represents the plots of illumination intensity vs photosensitivity for all the cells prepared with films doped with 0.001 M, 0.003 M, 0.005 M, 0.007 M, 0.009 M and 0.011 M of copper. Similar to the undoped cells, the photosensitivity increases as the intensity of illumination increases. The magnitude of photosensitivity is increased by two orders when compared to undoped cells. Also, it is observed from the figure, as the copper concentration increases for a particular intensity of illumination and for a particular annealing temperature, the corresponding photosensitivity increases and it reaches a maximum when the copper concentration is 0.005 M and then decreases. Hence, further studies were made only on the films with this doping concentration.

The incorporation of copper impurity in the CdS films decreased the dark conductivity. Due to the dual nature of copper impurity, the holes and electrons may recombine with majority carriers in the dark and minority carriers under illumination, thereby increasing the photosensitivity of the cell. In fact studies of copper diffusion in CdS [24] have shown that copper can act both as an acceptor and as a donor depending on whether it occupies substitution or interstitial sites in the lattice. The acceptor dominant behaviour of copper arises when the number of copper ions on cadmium substitutional sites is larger than the number of atoms in the interstitial positions. It is clear from the results observed here that in the II–VI semiconducting compounds, copper is associated with photoconductivity sensitizing centers.

Copper centers are situated at 0.6 eV above the valence band as reported by Tyurn et al. [25]. The maximum photosensitivity is observed for the doping concentration of 0.005 M, which corresponds to 441 ppm of copper. AAS analysis of the Cu concentration corresponding to this doping revealed the presence of 405 ppm of copper. This particular concentration corresponds to a donor to acceptor ratio around unity. For other concentrations of copper doping, this ratio deviates from unity, and hence, the photosensitivity, decreases. The acceptor dominant behaviour of copper arises when the number of copper ions on Cd substitutional sites is larger than the number of atoms in the interstitial positions. Thus to fix the acceptor and donor concentrations as required above, the total donor concentration must be determined and distinction between electrically active impurities and crystal defects as a function of processing variables must be made.

Fig. 9 shows the variation in the photocurrent with illumination for both the undoped and the doped cells. As discussed earlier, the high photosensitivity associated with CdS arises due to the presence of compensated acceptors, which act as sensitizing centers. As the excitation intensity is increased, these centers become more active and the photosensitivity sharply increases at some region of excitation. It is observed from the figure, that up to 5000 lx, the photocurrent varies linearly with illumination, becoming super linear

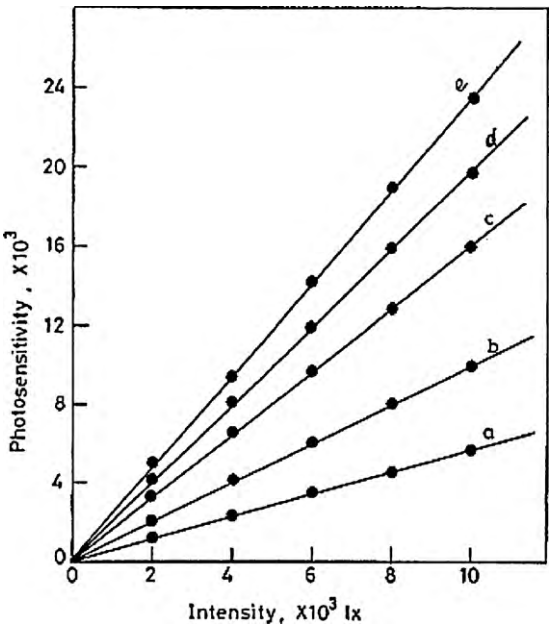

Fig. 7. Dependence of photosensitivity on illumination intensity for undoped CdS films deposited at a substrate temperature of 300 °C and post-heated in air at different temperatures: (a) 450 °C, (b) 475 °C, (c) 500 °C, (d) 525 °C and (e) 550 °C.

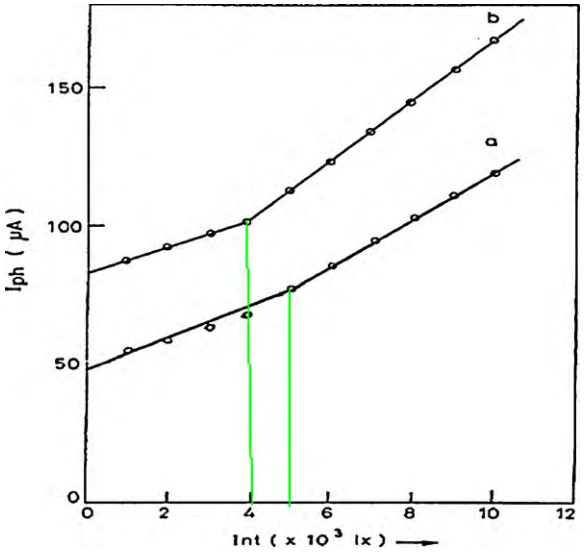

Fig. 9. Variation of photocurrent with illumination intensity of CdS films deposited at a substrate temperature of 300 °C and post-heated in air at 550 °C. (a) Undoped and (b) doped with copper (0.005 M).

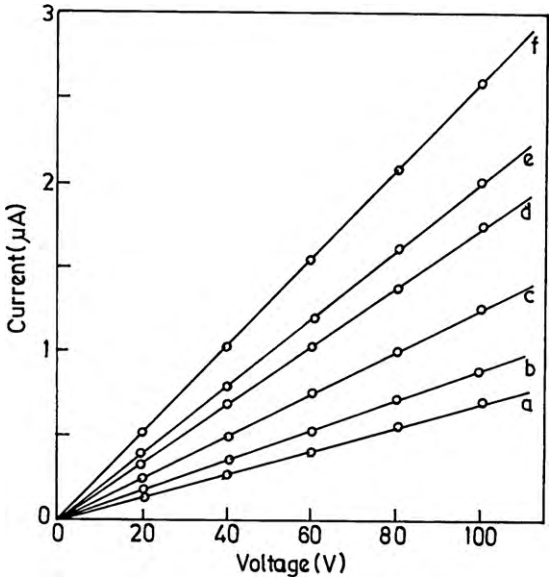

Fig. 10. Plots of current vs voltage of CdS films deposited at different substrate temperatures (a) 50 °C, (b) 100 °C, (c) 150 °C, (d) 200 °C, (e) 250 °C and (f) 300 °C.

above this intensity. But for the doped cells, linearity is observed up to 4000 lx and above this intensity super linearity is observed. The super linearity arises from the conversion of hole traps into recombination centers when the hole quasi Fermi level moves towards the valence band with an increase in light intensity. These recombination centers, which have higher capture cross-sections for the holes than electrons, in conjunction with another set of recombination centers with equal capture cross-sections for both the carriers, decrease the lifetime of the holes thereby increasing the lifetime of the electrons. While the hole traps are being converted into recombination centers, the electron lifetime is continuously increasing and the photocurrent varies super linearly with increasing light intensity [26]. The transition from linearity to super linearity occurs when the hole demarcation level is at the level of the recombination centers with equal capture cross-section. Similar results were observed in sprayed [27], vacuum evaporated [28] and single crystal CdSe [29]. The super linearity in CdSe occurs only when the Fermi level varies between 0.3 eV and 0.6 eV from the conduction band. Also it is reported [30] that the small time constants of highly photosensitive films have been attributed to the super linearity of CdSe at higher intensity of illumination. Current–voltage characteristics of the films deposited at different substrate temperatures are linear (Fig. 10).

Tables 3 and 4 present the signal to noise ratio (SNR) of the undoped CdS films deposited at different substrate temperatures and Cu doped films, respectively. It is observed that the SNR is found to increase gradually as the bias voltage increases and is found to be maximum for the films deposited at a substrate temperature of 300 °C. For the doped samples, SNR is maximum for a doping of 700 ppm of Cu. The SNR is higher for the doped films compared to undoped films.

Table 3
SNR of the CdS films deposited at different substrate temperatures (bias voltage: 170 V).

Substrate temperature (°C)	SNR
30	40
100	70
200	130
300	200

Table 4
SNR of the CdS films deposited at 300 °C substrate temperature and doped with copper of different concentrations (bias voltage: 170 V).

Copper concentration (ppm)	SNR
30	90
70	120
100	190
200	350

4. Conclusions

The results obtained in this investigation clearly indicate that CdS films exhibiting good photoconductive response and with high signal to noise ratio can easily be obtained by the electron beam evaporation technique. CdS films with direct bandgap of 2.39 eV can easily be obtained.

References

[1] I.L. Oladeji, C. Chow, V. Ferekides, V. Viswanathan, Z. Zhao, Sol. Energy Mater. Sol. Cells 61 (2000) 203.
[2] J.K. Dongre, M. Ramrakhiani, J. Alloys Compd. 487 (2009) 653.
[3] H. Khallaf, I.O. Oladeji, L. Chow, Thin Solid Films 516 (2008) 5967.
[4] J.S. Meth, S.G. Zane, K.G. Sharp, S. Agarwal, Thin Solid Films 444 (2003) 227.
[5] C.T. Tsai, D.S. Chuu, G.L. Chen, S.L. Yang, J. Appl. Phys. 79 (1996) 9105.
[6] S. Ikhmayies, R.N. Ahmad-Bitarb, J. Lumin. 128 (2008) 615.
[7] Z. Cheng, F. Su, L. Pan, M. Cao, Z. Sun, J. Alloys Compd. 494 (2010), L.7.
[8] G. Perna, V. Capozzia, S. Pagliara, M. Ambricob, D. Lojaconoa, Thin Solid Films 387 (2001) 208.
[9] R.N. Ahmad-Bitar, Renew. Energy 19 (2000) 579.
[10] K.P. Acharya, K. Mahalingam, B. Ullrich, Thin Solid Films 518 (2010) 1784.
[11] S.J. Ikhmayies, Production and characterization of CdS/CdTe thin film photovoltaic solar cells of potential industrial use, Ph.D. Thesis, University of Jordan, 2002.
[12] D. Cha, S. Kim, N.K. Huang, Mater. Sci. Eng. B 106 (2004) 64.
[13] J.H. Lee, D.J. Lee, Thin Solid Films 515 (2007) 6055.
[14] S. Soundeswaran, O. Senthil Kumar, S. Moorthy Babu, P. Ramasamy, R. Dhanasekaran, Mater. Lett. 59 (2005) 1795.
[15] B. Ullrich, R. Schroeder, IEEE J. Quantum Electron 37 (2001) 1363.
[16] Z. He, G. Zhao, W. Weng, P. Du, G. Shen, G. Han, Vacuum 79 (2005) 14.
[17] M. Khanlary, P. Townsenda, B. Ullrich, D.E. Hole, J. Appl. Phys. 97 (2005) 023512.
[18] F. Liu, Y. Lai, J. Liu, B. Wang, S. Kuang, Z. Zhang, J. Li, Y. Liu, J. Alloys Compd. 493 (2010) 305.
[19] K. Reichelt, X. Jiang, Thin Solid Films 191 (1990) 91.
[20] K.L. Chopra, Thin Film Phenomena, McGraw Hill, New York, London, 1969, p. 272.
[21] V. Kumar, B.S.R. Sastry, Cryst. Res. Technol. 36 (2001) 565.

[22] G. Perna, V. Capozzi, M.C. Plantamura, A. Minafra, P.F. Biagi, S. Orlando, V. Marotta, A. Giardini, Appl. Surf. Sci. 186 (2002) 521.
[23] P.K.R. Kalita, B.K. Sharma, D.L. Das, Bull. Mater. Sci. 23 (2000) 313.
[24] A. Rose, Concepts of Photoconductivity and Allied Problems, Wiley, NY, 1963.
[25] L.I. Tyurn, Yu.A. Varvas, Tr. Tallin, Politekhn. Inst. Ser. A 236 (1966) 39.
[26] H. Okhimura, Y. Sakai, Jpn. J. Appl. Phys. 7 (1968) 731.
[27] A.K. Raturi, R. Thangaraj, P. Rajaram, B.B. Tripathi, O.P. Agnihotri, Thin Solid Films 106 (1983) 257.
[28] R.H. Bube, Proceeding Conference Photoconductivity, Atlanta, 1954.
[29] A.K. Raturi, R. Thangaraj, P. Rajaram, B.B. Tripathi, O.P. Agnihotri, Thin Solid Films 91 (1982) 55.
[30] C.M. Lampert, R. Mark, Current Injection in Solids, Academic Press, NY, 1970.